2021 IEEE 21st International Conference on Nanotechnology (NANO)
July 28-30, 2021. Montréal, Canada

THE HYSTERESIS LOOP STUDIES OF MAGNETIC TUNNEL JUNCTION-BASED MOLECULAR SPINTRONICS DEVICES (MTJMSD) EMPLOYING MONTE CARLO SIMULATIONS

Zafar Waqar, Bishnu R Dahal, Eva Mutunga, Marzieh Savadkoohi, Uzma Amir, Pius Suh, Hayden Brown, Andrew Grizzle, Christopher D'Angelo, and Pawan Tyagi

***Abstract*— The hysteresis loop investigations of different size magnetic tunnel junction molecular spintronics devices (MTJMSD) have been done by Monte Carlo simulation (MCS). We employed a continuous MCS algorithm to investigate single-molecule magnet SMM's spin state's impact as a function of molecular exchange coupling strength. The applied magnetic fields were ramped at a variety of ranges of increments, unfolding physics behind the magnetization nature of each MTJMSD. The magnetic moment changes with applied magnetic fields exhibit the characteristics of devices being studied. The MTJMSDs were studied for ferromagnetic and antiferromagnetic exchange couplings. The magnetic moment saturation, retentivity, coercivity, and permeability are studied.**

I. INTRODUCTION

This There have been a range of hysteresis loop (HL) studies of bulk magnets and thin magnetic films ranging from a long ago[1] to a few decades ago[2–6]. There are important investigations of hysteresis loop area (HLA) as a function of the applied magnetic field frequency and amplitude for thin magnetic films[7-9]. The studies of the HLA were reported in the pioneering work1 for 3D magnets. There are keynote 2D HL studies for thin ferromagnetic films[10-13] where mean field type models with single[10] or many[11] relaxation times were applied to characterize the experimental data. Those studies considered that the HL was being controlled by the nucleation process, predicting logarithmic dependence of the coercive field on the rate of the applied magnetic field. In an experimental study[9] it was found that HLA changes with frequency of applied field as a small exponent ($\sim 0.03-0.06$) or, possibly, logarithmically.

There are some studies on molecular spintronics devices (MSDs) as a viable candidate for futuristic advanced detecting sensors, devices and quantum computational applications[14-16]. The organometallic molecules[17] have attracted some researchers to employ these molecules as the device element in futuristic MSDs. For MSD fabrication, the organometallic clusters are required to be connected with a source and drain-type metal electrodes[18] at least. The intensity of molecular bonding with electrodes will depend on the type of bonding[19]. A molecule with a functional group like sulfur can form covalent or ionic bonds, which provide very strong coupling[20, 21] to demonstrate strong hybridization of energy levels[22], specifically in case of covalent bonding. The resulting strong hybridization gives rise to novel features for metal electrodes and organic molecules. The thiolate molecule has been found to produce magnetism in non-magnetic electrodes[23]. A molecule connected to some metal electrodes will exhibit new properties rather than its own signature properties in isolated state. So, the combined system of metal electrodes and molecules becomes a new composite system[23, 24]. Study of such composite systems in the field of MSD is crucial while having single molecular magnets (SMM) like molecules possessing a widespread range of spin states interacting with magnetic electrodes[23]. Strong long-range coupling is observed from magnetic electrodes, like nickel (Ni), cobalt (Co), and iron (Fe). Our earlier experimental studies showed that Mn hexanuclear[25] and Fe-Ni octanuclear molecular complexes(OMC)11 based SMM happen to produce long-range impacts on ferromagnetic electrodes leading to room temperature observations of several orders of magnitude current suppression, spin photovoltaic effects, and several temporary orders of magnitude magnetoresistance[25, 26]. There are similar other studies like that of strong coupling between C60 molecules and ferromagnetism of the nickel electrodes leading to the Kondo splitting phenomenon without applying the estimated ~50 T field needed for this observation[27]. Fabricating a complete MSD is a big challenge even after having experimentally determined the spin states of paramagnetic molecules. The Density Function Theory (DFT) methodology approach has its limitation and is indeed challenging to simulate SMM-connected to actual large-scale MSDs with long ferromagnetic electrodes[28]. This paper reports on MCS study of HL. The first part of the study is to investigate the effects on hysteresis loop due to changing applied magnetic field increment counts. The second part of the study is to apply parallel and anti-parallel magnetic moments left and right electrode and study the effects on hysteresis loop. We employed the Heisenberg Model[29] of MTJMSD that had shown promising results in our prior MCS[30]. This paper provides new insights into MTJMSD magnetic flux and other characteristics changing due to changing driving key parameters.

II. METHODOLOGY

We utilized a continuous spin model to select spin vectors of the ferromagnets' atoms and molecules to assume changed directions in spherical coordinate system[31]. The

*We gratefully acknowledge the funding support from National Science Foundation-CREST Award (Contract # HRD- 1914751), and Department of Energy/National Nuclear Security Agency (DE-FOA-0003945). (Corresponding author Pawan Tyagi, email: ptyagi@udc.edu)

three dimensions of an MTJMSD model are governed by the indices representing height (H), width (W), and length (L). The MTJMSD's dimension is represented by H × W × L. To represent the molecules on the edges, a plane containing atoms along the perimeter and with the empty interior was introduced between the two FM electrodes of equal volume. The molecular plane is inserted along the H dimension of an MTJMSD. The inter-FM electrode magnetic coupling is only occurring via the molecules. However, inter-FM electrode coupling via the empty region is set to zero. We performed MC simulations by varying molecular coupling strength with the left FM (JmL) and right FM (JmR) electrodes, kT, and MTJMSD dimensions. For our current studies, we focused on Heisenberg model (Fig.1e) as a 3D analogue of an MTJMSD (Fig. 1b)[27]. In this MCS study we represented tunnel barrier with an empty space within a square shaped molecular perimeter (Fig.1f). The molecular perimeter was a 5x5 square with molecular analogs. In Fig.1f we have shown 4x4 molecular square to produce an illustration. The paramagnetic SMM molecules of MTJMSD (Fig.1d) were represented by the atomic scale analog with adjustable spin parameter. The coupling between two FM electrodes were only caused by the paramagnetic molecules (Fig. 1f). Molecule mediated exchange coupling with the left and right FM electrodes is governed by the molecule coupling with left electrode (JmL) and molecule coupling with the right electrode (JmR), respectively. JL, and JR, are the Heisenberg exchange coupling strengths for the left and right FM electrodes (Fig. 1b). In our MCSs the atoms beyond boundary of MTJMSD model (Fig. 1b) were set with zero spin state[32]. More details of our MCS are published elsewhere11. The units of total energy and exchange coupling parameters are the same as of kT. In this study, the exchange coupling parameters and kT are referred to as the unitless parameters. The overall magnetic moment of the MTJMSD is the sum of the magnetic moment of the molecules, left FM, and right FM electrodes. In the 1st part of our studies, we kept all parameters fixed and changed only applied magnetic field increment counts and changed in orders of magnitude to get resulting hysteresis loop changes. In the 2nd part we have mainly focused of the molecule induced strong ferromagnetic and strong antiferromagnetic coupling with JmL and JmR being 1,1 and 1, -1 respectively.

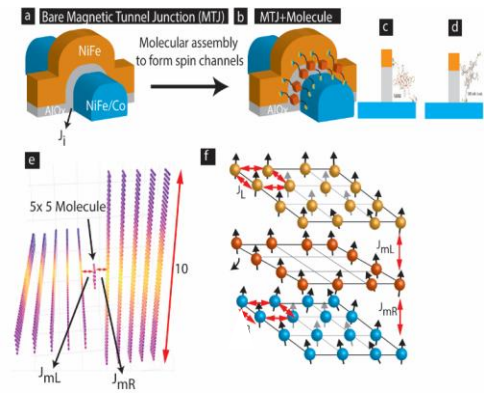

Figure 1. MSD formed by utilizing exposed edges of (a) Bare MTJ to attach (b) paramagnetic molecules between two ferromagnets. (c) SMM and (d) OMC paramagnetic molecules connected to ferromagnets via sulfur atom. (e) An illustration of a 3D Heisenberg Model of a Molecular device. (f)) Exchange coupling parameters associated with molecule-ferromagnet interactionscaption.

JmL, and JmR, are the Heisenberg exchange coupling strengths for the for molecule to left and to right FM electrodes, respectively. In our MCSs the atoms beyond boundary of MTJMSD model were set with zero spin state[32]. More details of our MCS are published elsewhere[11]. The units of total energy and exchange coupling parameters are the same as of kT. In this study, the exchange coupling parameters and kT are referred to as the unitless parameters. The overall magnetic moment of the MTJMSD is the sum of the magnetic moment of the molecules, left FM, and right FM electrodes. In the 1st part of our studies, we kept all parameters fixed and changed only applied magnetic field increment counts and changed in orders of magnitude to get resulting hysteresis loop changes. In the 2nd part we have mainly focused of the molecule induced strong ferromagnetic and strong antiferromagnetic coupling with JmL and JmR being 1,1 and 1, -1 respectively. To make this study generic we also varied molecular coupling strength, thermal energy, molecular spin state, and MTJMSD dimensions.

The template is used to format your paper and style the text. All margins, column widths, line spaces, and text fonts are prescribed; please do not alter them. You may note peculiarities. For example, the head margin in this template measures proportionately more than is customary. This measurement and others are deliberate, using specifications that anticipate your paper as one part of the entire proceedings, and not as an independent document. Please do not revise any of the current designations.

III. RESULTS AND DISCUSSION

Detailed hysteresis loop MCS studies done on an array of different size MTJMSD produced datasets with different parameters. We started from 11 x 10 x 10, size MTJMSD and increased device sizes and accordingly applied range of magnetic fields, getting different hysteresis loops. For bigger size devices, having been applied smaller magnetic field, we got asymmetric hysteresis loops and no saturation for the magnetic moment on either side of the hysteresis loop. On the other hand, on small size devices, having applied higher magnetic field, MSC produced perfectly symmetric hysteresis loops with magnetic moment saturation attained and no change in magnetic moment for increasing magnetic field. In order to get a similar symmetric hysteresis loop for a bigger size device, the applied magnetic field had to be increased. For a particular size device, an ideal applied magnetic field range is found from our MCS simulations. Here in this paper, we present detailed investigations of two categories of MCS investigation. The first MCS studies were of different MTJMSD hysteresis loops carried out with magnetic field

ramped with different orders of magnitude increment counts. The second MCS studies were of different MTJMSD hysteresis loops carried out with parallel and anti-parallel magnetic moments coupling. The resulting MCS of the studied MTJMSD revealed different shapes of hysteresis loops. In order to get in-depth detailed insight of the characteristics independently of our MTJMSD, we kept all other parameters unchanged while ramping only one parameter at a time as described below under each section.

A The effect of Different increment counts:

For different MTJMSD, the magnetic fields were ramped in different number of count increments to get nature of the physics behind obtained symmetric and asymmetric hysteresis loops. The total magnetic flux was found to be almost same in both positive and negative directions for all cases of increments counts of the applied magnetic fields. The retentivity for magnetic field was found changing with changed applied magnetic field ramped with different increment counts, decreasing with increasing the number of increment counts. The hysteresis loops of MTJMSD of size 11 x 10 x 10 for applied magnetic field with increments counts 10^{-6}, 10^{-7}, 10^{-8} and 10^{-9} are shown in Fig. 2. For increments counts 10^{-6} applied of the net magnetic field, the net magnetic retentivity is 477 whereas for applied net magnetic field with increments counts of 10^{-7}, 10^{-8} and 10^{-9} magnetic retentivity is 403, 266 and 108 respectively. The total magnetic flux in the four cases is 500, 501, 503 and 503, respectively, and it was found to be changing significantly with changing the MTJMSD sizes and those investigations of device size changes are not being reported here.

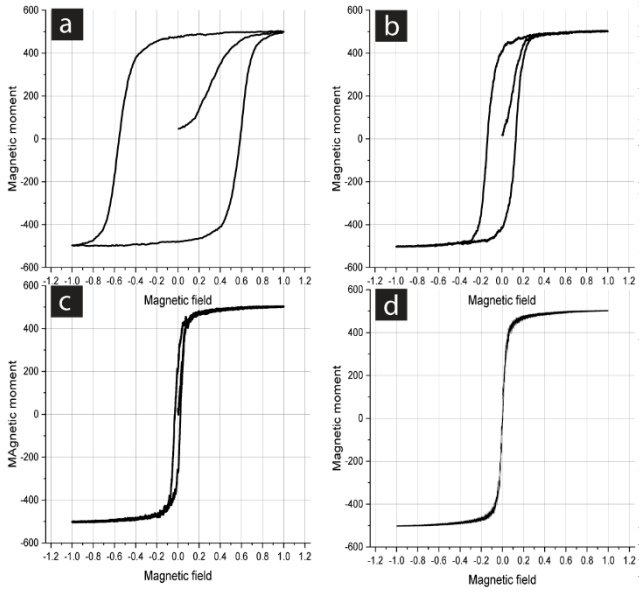

Figure 2. Hysteresis loop of MTJMSD, magnetic field with 10^{-6}, 10^{-7}, 10^{-8} and 10^{-9} increment counts ramped.

For increment counts of 10^{-6}, 10^{-7}, 10^{-8} and 10^{-9} applied magnetic field, the corresponding coercivity is 0.55, 0.14, 0.023 and around 0 respectively. The change in coercivity upon change in increment counts of applied magnetic field is significant an order of magnitude change in increment counts of the applied magnetic field results in significant change in coercivity. This significant change in coercivity is due to increased time of applied magnetic field uniformly ramped, exhibiting the MTJMSD a ferromagnetic material.

B Magnetic moment orientation effect

For a MTJMSD of size 11 x 10 x 10 for 0.1 applied magnetic field in positive and negative direction with increment counts of 10^{-9}. while magnetic moment of left electrode JmL and of right electrode JmR being same (1, 1) or opposite (1, -1) the obtained MCS are shown in Fig. 3a, b respectively.

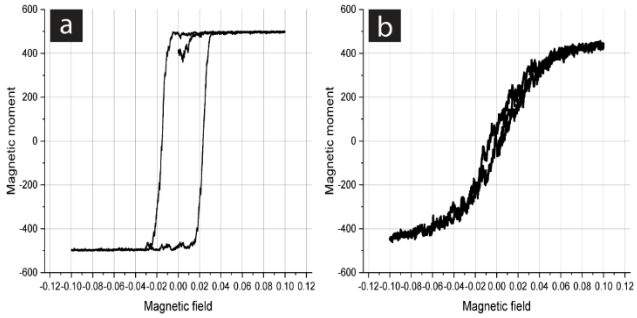

Figure 3. Hysteresis loop of MTJMSD, magnetic field with 10^{-9} increment counts for (a) JmL, JmR parallel coupling and (b) JmL, JmR anti-parallel coupling.

When the two electrodes are set to aligned in the same direction then hysteresis loop widens for positive and negative values of the applied magnetic field as shown in Fig. 3a, depicting considerable magnetic coercivity. As for retentivity, in case of two electrodes having parallel coupling the magnetic retentivity is 488 while in case of two electrodes being anti-parallel (as shown in Fig. 3b) the retentivity is around zero, showing a soft magnetic behavior. The net magnetic flux in case of magnetic moments being parallel and anti-parallel is significantly different, 980 in case of parallel couplings and 453 in case of anti-parallel couplings. The overall hysteresis loop's slope is rather sharp in case of parallel couplings, giving a soft magnet trend as compared to relatively hard magnet trend in case of anti-parallel coupling. More detailed and systematic MCS investigations coupled with experimental studies are required to reveal the rout cause of this effect and make predictions for future device applications usage of this novel phenomenon.

The two extreme cases of magnetic moments being parallel and anti-parallel provides us this very important parameter to tweak for specific device applications to get desired threshold magnetization. So, we plan to investigate case of two electrodes being partially parallel and anti-parallel to each other in our future MCS.

IV. CONCLUSION

Our MCS studies have provided new insight into the nature and behavior of magnetization of the studied MTJMSD. With change of applied magnetic field increments counts, we found compelling change in magnetic coercivity, gradually decreasing with increased increment counts of the applied magnetic field. On the other hand, the total magnetic flux remained unchanged due to increments count change of the applied magnetic field. So, the net magnetic flux is the prime signature of a particular size MTJMSD, and size of the device will dictate the change in net magnetic flux, while magnetic coercivity and retentivity will change with change of increment counts change of the applied magnetic field. The magnetic retentivity also changes with changing the increment counts change of the applied magnetic field, decreasing with increasing the applied magnetic field increment counts. Our MCS studies have additionally confirmed our earlier theoretical and experimental studies showing molecules establishing ferromagnetic coupling with one electrode and antiferromagnetic coupling with the other electrode The overall antiferromagnetic and ferromagnetic coupling behavior demonstrates in accordance with our recently reported results that paramagnetic single molecular magnet SMM made antiferromagnetic and ferromagnetic coupling to the first electrode and ferromagnetic coupling to the second ferromagnetic electrode, respectively. Our current investigations complement our earlier published results providing valuable information for the future generation of quantum computing and other applications.

REFERENCES

[1] C.P.Steinmetz, Trans.Am.Inst.Electr.Eng. 9, 3 (1892).
[2] W.S.Lo and R.Pelcovits Phys.Rev.A 42, 7471 (1990).
[3] D.Dhar and P.B.Thomas, J.Phys.A 25, 4967 (1992).
[4] M.Acharyya and B.K.Chakrabarti, Physica A 192, 471 (1993); Phys.Rev.B 52, 6550 (1995).
[5] C.N.Luse and A.Zangwill, Phys.Rev.E 50, 224 (1994).
[6] M. Rao, H. R. Krishnamurthy and R. Pandit, J. Phys. C 1, 9061 (1989).
[7] Y.L.He and G.C.Wang, Phys.Rev.Lett. 70, 2336 (1993).
[8] Q.Jiang, H.-N.Yang, and G.C.Wang, Phys.Rev.B 52, 14911 (1995).
[9] J.-S.Suen and J.L.Erskine Phys.Rev.Lett. 78, 3567 (1997).
[10] P.Bruno, G.Bayreuther, P.Beauvillain, C.Chappert, G.Lugert, D.Renard, J.P.Renard, and J.Seiden, J.Appl. Phys. 68, 5759 (1990).
[11] B.Raquet, R.Mamy, and J.C.Ousset Phys.Rev.B 54, 4128 (1996).
[12] J. Chen and J.L. Erskine, Phys. Rev. Lett. 68, 1212 (1992).
[13] W. Weber, C.H. Back, A. Bischof, D. Pescia, and R. Allenspach, Nature 376, 788 (1995).
[14] Bogani and W. Wernsdorfer, Nat. Mater. 7 (3), 179-186 (2008).
[15] D. F. Li, S. Parkin, G. B. Wang, G. T. Yee, R. Clerac, W. Wernsdorfer and S. M. Holmes, J. Am. Chem. Soc. 128 (13), 4214-4215 (2006).
[16] M. Fonin, S. Voss, S. Herr, G. de Loubens, A. D. Kent, M. Burgert, U. Groth and U. Rudiger, Polyhedron 28 (9-10), 1977-1981 (2009).
[17] D. F. Li, C. Ruschman, R. Clerac and S. M. Holmes, Inorg. Chem. 45 (13), 7569 (2006).
[18] T. Li, W. P. Hu and D. B. Zhu, Adv. Mater. 22 (2), 286-300 (2010).
[19] J. M. Seminario, C. E. De la Cruz and P. A. Derosa, J. Am. Chem. Soc. 123 (23), 5616-5617 (2001).
[20] H. B. Heersche, Z. de Groot, J. A. Folk, H. S. J. van der Zant, C. Romeike, M. R. Wegewijs, L. Zobbi, D. Barreca, E. Tondello and A. Cornia, Phys. Rev. Lett. 96 (20), 206801 (2006).
[21] P. Tyagi, D. F. Li, S. M. Holmes and B. J. Hinds, J. Am. Chem. Soc. 129 (16), 4929-4938 (2007).
[22] M. Galbiati, Molecular Spintronics : From Organic Semiconductors to Self-Assembled Monolayers. (Springer International Publishing, Switzerland, 2015).
[23] F. Al Ma'Mari, T. Moorsom, G. Teobaldi, W. Deacon, T. Prokscha, H. Luetkens, S. Lee, G. E. Sterbinsky, D. A. Arena, D. A. MacLaren, M. Flokstra, M. Ali, M. C. Wheeler, G. Burnell, B. J. Hickey and O. Cespedes, Nature 524 (7563), 69-U128 (2015).
[24] P. Tyagi, C. Baker and C. D'Angelo, Nanotechnology 26, 305602 (2015).
[25] P. Tyagi, C. Riso, U. Amir, C. Rojas-Dotti and J. Martínez-Lillo, RSC Advances 10 (22), 13006-13015 (2020).
[26] P. Tyagi and C. Riso, Organic Electronics 75, 105421 (2019).
[27] A. N. Pasupathy, R. C. Bialczak, J. Martinek, J. E. Grose, L. A. K. Donev, P. L. McEuen and D. C. Ralph, Science 306 (5693), 86-89 (2004).
[28] K. Park and H. S. M., Phys. Rev. B 74, 224440 (2006).
[29] A. Grizzle, C. D'Angelo and P. Tyagi, AIP Advances 11 (1), 015340 (2021).
[30] M. Savadkoohi, B. R. Dahal, A. Grizzle, C. D'Angelo and P. Tyagi, Journal of Magnetism and Magnetic Materials 529, 167902 (2021).
[31] M. E. Newman and G. T. Barkema, Monte Carlo Methods in Statistical Physics. (Clarendon Press, Oxford, 1999).
[32] M. E. Newman and G. T. Barkema, Monte Carlo Methods in Statistical Physics. (Clarendon Press, Oxford, 1999).